3-31-2016

Fine-scale spatial ecology drives kin selection relatedness among cooperating amoebae

jeff smith

Joan E. Strassmann
Washington University in St Louis, strassmann@WUSTL.EDU

David C. Queller
Washington University in St Louis, queller@WUSTL.EDU

EVOLUTION
INTERNATIONAL JOURNAL OF ORGANIC EVOLUTION

Fine-scale spatial ecology drives kin selection relatedness among cooperating amoebae

Journal:	*Evolution*
Manuscript ID	15-0339.R2
Manuscript Type:	Original Article
Date Submitted by the Author:	09-Feb-2016
Complete List of Authors:	smith, jeff; Washington University in St Louis, Biology Strassmann, Joan; Washington University in St. Louis, Biology; Queller, David; Washington University, Department of Biology;
Keywords:	Population Structure, Selection - Group/Kin, Sociality

Fine-scale spatial ecology drives kin selection relatedness among cooperating amoebae

jeff smith*, Joan E. Strassmann, and David C. Queller

Department of Biology, Washington University in St. Louis, Saint Louis, MO 63130, USA
* Corresponding author: jeffsmith@wustl.edu

Running head: Spatial ecology of relatedness in social amoeba

Keywords: altruism / cooperation / dispersal / relatedness / spatial structure

Data archiving: Data and analysis scripts will be made publically available in the Dryad.org public database upon acceptance. We will also make these available to reviewers, if desired.

Abstract

Cooperation among microbes is important for traits as diverse as antibiotic resistance, pathogen virulence, and sporulation. The evolutionary stability of cooperation against "cheater" mutants depends critically on the extent to which microbes interact with genetically similar individuals. The causes of this genetic social structure in natural microbial systems, however, are unknown. Here we show that social structure among cooperative *Dictyostelium* amoebae is driven by the population ecology of colonization, growth, and dispersal acting at spatial scales as small as fruiting bodies themselves. Despite the fact that amoebae disperse while grazing, all it takes to create substantial genetic clonality within multicellular fruiting bodies is a few millimeters distance between the cells colonizing a feeding site. Even adjacent fruiting bodies can consist of different genotypes. Soil populations of amoebae are sparse and patchily distributed at millimeter scales. The fine-scale spatial structure of cells and genotypes can thus account for the otherwise unexplained high genetic uniformity of spores in fruiting bodies from natural substrates. These results show how a full understanding of microbial cooperation requires understanding ecology and social structure at the small spatial scales microbes themselves experience.

Introduction

Microbes cooperate in many ways, from signaling (West et al. 2012; Pollitt et al. 2014) to pathogenesis (Raymond et al. 2012; Diard et al. 2013; Pollitt et al. 2014) to antibiotic resistance (Yurtsev et al. 2013). At the same time, microbial "cheaters" that benefit from cooperative traits without contributing to them are common and play a role in disease systems (Raymond et al. 2012; Diard et al. 2013; Pollitt et al. 2014). Whether natural selection favors cooperation or cheating depends critically on the statistical similarity of interacting individuals at loci affecting those traits—what kin selection theory calls "relatedness" (Hamilton 1964; Grafen 1985; Queller 1992). Kin selection relatedness is a regression coefficient that measures the similarity of social partners above and beyond similarity to the average competitor in their population. But where does relatedness come from in microbes, and what determines how much of it there is?

Spatial proximity can sometimes serve as a proxy indicator of genetic similarity. Animals, for example, often direct cooperative behaviors to classes of individuals (such as nestmates) whose proximity indicates they are likely to be close genealogical kin. Similarly, microbes often live in environments where they form microcolonies or biofilms in which neighboring cells are often clonemates. A large part of social structure in microbes is then the distribution of strains among groups of interacting cells (smith et al. 2010) which is in turn determined by the population ecological processes of group formation, group dissolution, and migration of cells between groups. In principle, microbial social structure is determined by everything that affects the statistical similarity of interacting individuals. Other important processes include diffusion of extracellular products (Kümmerli et al. 2009), production of and response to chemical signals (West et al. 2012; Pollitt et al. 2014), meiotic recombination and reassortment, horizontal gene transfer (Dimitriu et al. 2014), and exclusion of unlike individuals (Strassmann et al. 2011). Laboratory experiments have shown that all these processes can in principle promote relatedness and the evolution of cooperation, but how important they are in natural microbial habitats remains unknown.

A prominent model system for microbial cooperation is the cellular slime mold *Dictyostelium discoideum* (Strassmann and Queller 2011). These amoebae graze on bacteria in forest soil and fecal droppings. When starved, *D. discoideum* cells aggregate and form multicellular fruiting bodies. Some cells become stress-resistant spores. Others cells form a stalk that holds the spore mass aloft, increasing their likelihood of being carried to new

feeding sites by arthropods (smith et al. 2014). Stalk cells die after creating the cellulose-based structure of the stalk, so stalk production is a form of microbial altruism. Cheater mutants are able to preferentially become spores in mixed-genotype fruiting bodies with wild-type cells (Santorelli et al. 2008) despite sometimes being unable to form fruiting bodies on their own (Ennis et al. 2000; Gilbert et al. 2007; Kuzdzal-Fick et al. 2011). Cheater mutants spread quickly in populations with low relatedness (Kuzdzal-Fick et al. 2011). Natural *D. discoideum* isolates also contribute different proportions of cells to spore or stalk when forming fruiting bodies with other genotypes than when on their own (Strassmann et al. 2000; Buttery et al. 2009), in large part due to production of and response to substances secreted during development (Parkinson et al. 2011).

In this system, kin selection relatedness largely measures how clonal fruiting bodies are. Fruiting bodies grown from intact field-collected deer pellets are predominantly composed of single genotypes, with net relatedness 0.86–0.99 at microsatellite loci (Gilbert et al. 2007). This has been puzzling, however, because there is extensive genetic diversity at the millimeter scales over which cells aggregate into fruiting bodies. In one study, 6 mm diameter soil cores with *D. discoideum* contained more than one genotype 63% of the time (Fortunato et al. 2003). Allelic similarity of co-occuring haplotypes can account for ~0.5 relatedness, but the rest remains unexplained. Some Dictyostelid species have a form of kin recognition that causes different genotypes to segregate out into separate fruiting bodies during development (Mehdiabadi et al. 2006; Ostrowski et al. 2008; Benabentos et al. 2009), but in *D. discoideum* the effect is too weak to account for the strong genetic structure observed among fruiting bodies (Gilbert et al. 2012). The causes of genetic uniformity in *D. discoideum* fruiting bodies thus remain unknown.

Here we test the hypothesis that high degree of clonality within *D. discoideum* fruiting bodies is driven by fine-scale spatial demography. In microbes, the population ecology of colonization, proliferation, and dispersal can structure the distribution of genotypes at very small spatial scales (Nadell et al. 2010). Dictyostelid amoebae disperse while grazing on bacteria, but if the genotypes that colonize a feeding site are sufficiently distant from each other then most of the fruiting bodies they eventually form will only contain a single genotype. The strength of this effect, however, depends on how much cells actually disperse. And since cells can aggregate from an area a few millimeters diameter (Waddell 1982), it's unclear *a priori* whether this process is strong enough to generate high clonality in fruiting bodies in the face of millimeter-scale genetic diversity. Here we measure how

much amoebae disperse while grazing, how separated colonizers need to be to create high clonality in fruiting bodies, and assess whether these conditions are likely to occur in natural *D. discoideum* populations.

Methods

Strains

Dictyostelium discoideum strains NC28.1 and NC34.1 are wild-type (*wt*) natural isolates described previously (Francis and Eisenberg 1993). We obtained labeled derivatives of these strains from N. Buttery (Buttery et al. 2012), who transformed them with an integrable plasmid expressing red fluorescent protein (*rfp*) and the *neoR* antibiotic resistance gene (Pang et al. 1999). We obtained a strain of *Klebsiella pneumoniae* bacteria with spontaneous resistance to the antimicrobial G418 from N. Buttery. We stored all strains at –80 °C in 20% (v/v) glycerol.

Plaque growth

We quantified the spatial scale of amoeba population growth and dispersal while grazing by measuring plaque growth on *K. pneumoniae* lawns. We grew lawns on SM plates for 3 days, resuspended bacteria with 1.0 ml KK2, then let plates dry. In the middle of these plates we spotted 10^4 spores suspended in 10 µl KK2. We incubated plates at 22 °C with passive humidity and constant overhead light. As plaques grew, we marked the outermost visible position of amoebae among bacteria and the outer boundary of cell aggregates (Fig. 1A). We measured the radius of these edges as the mean of four evenly-spaced outward transects. We replicated experiments on different days using spores independently grown from frozen stocks.

We analyzed plaque growth data using nonlinear mixed effects models fit via maximum likelihood using the *nlme* package in *R*. Our data fit the dynamics expected of two-dimensional microbial growth under reaction-diffusion dynamics (Murray 2003), so we modelled plaque growth as $x = v_{\max}(t - t_0)(1 - e^{-a(t-t_0)})$, where the radius x of a plaque edge is a function of time t with a maximum linear growth rate $v_{\max}$ to which it accelerates at rate a. t_0 is the time at which a plaque edge first appears. We modeled individual

replicate plates as a random effect on v_{max} and t_0. We tested variation among genetic background in plaque growth using likelihood ratio (LR) tests on models fit with and without an additional fixed background effect on v_{max} and/or t_0. We had no *a priori* expectation for the dynamics of plaque feeding edges (the radial distance between the outermost visible sign of amoebae among bacteria and the outermost developmental aggregates), so we modelled it as a simple second-order polynomial around the mean sampling time. We included plate as a random effect on intercept, slope, and curvature. We tested for variation among backgrounds in boundary behavior using likelihood ratio tests on models fit with and without an additional fixed background effect on intercept, slope, and curvature.

Transect across plaques

To quantify the spatial scale of genotype assortment among fruiting bodies created by limited dispersal of amoebae in vegetative growth, we measured the genotype composition of spores from fruiting bodies sampled along a transect that crossed the intersection of two plaques from isogenic *wt*/*rfp* strain pairs. We let *K. pneumoniae* lawns grow on SM agar plates (Formedium, Hunstanton, UK) for 3 days, resuspended and replated cells with 1.0 ml KK2, and let dry. We spotted 10^4 *D. discoideum* spores in 10 µl KK2 onto lawns in two places 5.0 cm apart. We incubated plates at 22 °C with passive humidity and constant overhead light for 4–5 days, at which point plaques had grown together and fruiting bodies at the plaque intersection had finished developing. We sampled fruiting bodies as described above along a transect that connected the original sites of spore deposition, picking one fruiting body at each end plus seven at 3 mm intervals spanning the observed plaque intersection. We determined the proportion of *rfp* spores in each fruiting body by flow cytometry (see below). We replicated experiments on different days using spores independently grown from frozen stocks.

We analyzed transect data using nonlinear mixed effects models fit with the *nlme* package in *R*. Using maximum likelihood we fit asymptotic logistic curves of the form $y = a/(1 + e^{(x-b)/c})$, where y is the proportion *rfp* spores per fruiting body, x is a fruiting body's location along the transect, a is the asymptote, b is the midpoint, and c determines the slope around the midpoint. We modelled variation among plates as random effects on curve parameters and variation among *D. discoideum* backgrounds as fixed effects. We measured the statistical significance of model parameters using likelihood ratio tests on models fit

with and without the variable of interest. The location of plaque intersections varied from plate to plate, so to aid visualization we plotted the location of fruiting bodies along transects relative to the midpoint of the fitted curve for each plate.

Colonization density assay

To measure how colonization density and limited dispersal create spatial assortment of genotypes among fruiting bodies, we inoculated *K. pneumoniae* lawns with isogenic *wt*/*rfp* mixes of *D. discoideum* spores at several initial densities; allowed amoebae to graze, reproduce, and develop; and then quantified the distribution of *rfp* spores among fruiting bodies. *D. discoideum* is entirely asexual under these experimental conditions, creating complete linkage between the *rfp* locus and the rest of the genome, including loci that affect social behavior. We performed these experiments on relatively dense lawns to better reflect the bacteria-rich conditions of feces, where fruiting bodies are most easily found.

To obtain fresh spores with which to start experiments, we allowed amoebae to grow and develop on *K. pneumoniae* lawns on 35 ml SM agar (per liter: 10 g peptone, 10 g glucose, 1 g yeast extract, 1.9 g KH_2PO4, 0.6 g K_2HPO_4, 1.0 g $MgSO_4 \bullet 7H_2O$, 20 g agar) in 100 mm diameter plates incubated at 22 °C. For fluorescently labelled strains, we supplemented SM plates with 5 µg/ml G418 to select against spontaneous nonfluorescent mutants. We dislodged spores from fruiting bodies by banging plates upside down, and then harvested spores from the plate lid with 1.0 ml KK2 buffer (per liter: 2.25 g KH_2HPO_4, 0.67 g K_2HPO_4). We centrifuged spores 3 min at 3000 ×g, washed them once in 1.0 ml KK2 buffer, and resuspended them to a density of 5.0×10^6 cells/ml using spore counts in a cytometer. We mixed strains in equal volumes (200 µl each) and serially diluted the mixes in KK2. We measured the fraction of fluorescent spores in these initial mixes using flow cytometry (see below). We also performed experiments in which spores were either all fluorescent or all nonfluorescent.

To start the experiments, we spread 100 µl of a stationary phase SM broth culture of *K. pneumoniae* onto 35 ml SM plates containing no G418 and let them grow for 3 days at 22 °C, resulting in lawns with $\sim 10^7$ bacteria/mm^2. We then added *D. discoideum* such that plates began with 10^2, 10^3, 10^4, 10^5, or 10^6 spores (0.018, 0.18, 1.8, 18, or 180 spores/mm^2). We suspended bacteria and spores in 1 ml KK2 using a sterile glass spreader, spread them evenly across the plates, and allowed the plates to dry. We incubated plates at

22 °C with passive humidity and direct overhead light. Where possible, we determined the number of germinating spores by counting visible plaques after 3 days incubation.

After amoebae consumed the entire bacterial lawn and finished creating fruiting bodies (5–8 days), we collected spores from individual fruiting bodies with an ethanol-sterilized dissecting pin into 150 µl KK2 with 0.1% NP-40 detergent. We collected spores from 12 fruiting bodies at pre-determined locations dispersed across the plate. We then used spore samples for flow cytometry as described below. We replicated experiments on different days using spores independently grown from frozen stocks.

Microscopy

To visualize the spatial distribution of *rfp* and *wt* cells, we acquired white light and red fluorescent images of plates using a Zeiss SV11 stereomicroscope (Carl Zeiss Microscopy LLC., Thornwood NY, USA). We acquired greyscale images using AxioVision v4.9.1.0 (Carl Zeiss Microscopy LLC., Thornwood NY, USA) then aligned and merged these images into panoramas using Hugin v2012.0.0 (http://hugin.sourceforge.net). Images were uniformly adjusted for black and white levels, leaving intensity on a linear scale. We created false-color composite images using the "color" blending mode in Adobe Photoshop v11.0.2 (Adobe Systems, San Jose CA, USA). All images are of plates with strains NC28.1 and NC28.1 *rfp*.

Flow cytometry

We measured the number of fluorescent and nonfluorescent spores in individual fruiting bodies using a BD Accuri C6 flow cytometer (BD Biosciences, San Jose CA, USA). For each sample, we analyzed 30-35 µl at a flow rate of 66 µl/min. We exported data as .fcs files for analysis in the *R* statistical computing environment using Bioconductor (Gentleman et al. 2004) packages *flowCore*, *flowStats*, and *flowViz*. We analyzed files in batches that included all fruiting bodies sampled from a plate. We asinh-transformed all data, screened forward scatter (FSC-H) and side scatter (SSC-H) data for non-cellular debris, and gated for spores by fitting a bivariate normal distribution then including all events in the ±2.5 std. dev. region (Fig. S1A). This analysis identified a median 4.9×10^4 spores sampled per fruiting body, with most having between 10^4 and 4.9×10^4 spores (Fig. S2). We normalized red fluorescence (FL3-H) data from these events to align peaks from *rfp* and *wt* cells and

then algorithmically divided cells into two populations (Fig. S1B). In cases where the algorithm failed to identify the *rfp* and *wt* peaks, we analyzed data files in batches that included those from another plate in the same replicate with the same *rfp* strain. These analyses produced counts of *rfp* and *wt* spores that we used in further analyses. While we did observe some loss of fluorescence in *rfp*-only controls, most deviations from 50% *rfp* in the relatedness assay were caused by variation among experimental blocks in the initial percentage among germinating colonizers (Fig. S3).

Social structure

In the colonization density experiment, we quantified the distribution of genotypes among fruiting bodies in terms of Hamilton's *r*—the regression coefficient of average neighbor genotype on individual genotype (Queller 1992). In kin selection theory, this is the relatedness within fruiting bodies at the *rfp* locus relative to the population on the plate. We used the estimator of Queller & Goodnight (1989), modified to measure whole-group relatedness (i.e. including one's self in the group) (Pepper 2000). That is, it measures the quantity that is important for kin selection: the probability that members of a common fruiting body are identical at the locus, above and beyond how identical they would be with random grouping on the plate. If we let n_{rfp} and n_{wt} be the total numbers of *rfp* and *wt* spores sampled from fruiting body g and let p_{rfp} and p_{wt} be their proportions in fruiting body g, then the regression coefficient is

$$r = \frac{\sum_{g}\left[n_{\mathrm{rfp}}(p_{\mathrm{rfp}} - \bar{p}_{\mathrm{rfp}(-g)}) + n_{\mathrm{wt}}(p_{\mathrm{wt}} - \bar{p}_{\mathrm{wt}(-g)})\right]}{\sum_{g}\left[n_{\mathrm{rfp}}(1 - \bar{p}_{\mathrm{rfp}(-g)}) + n_{\mathrm{wt}}(1 - \bar{p}_{\mathrm{wt}(-g)})\right]} \qquad (2)$$

where $\bar{p}_{\mathrm{rfp}(-g)}$ and $\bar{p}_{\mathrm{wt}(-g)}$ are estimates of the population-wide frequencies of *rfp* and *wt* spores that correct for downward bias with small sample sizes by making the calculation among all fruiting bodies other than g (Queller and Goodnight 1989). This formulation of *r* is equivalent to F_{ST} measured at the *rfp* locus where individual fruiting bodies are subpopulations within the total population of spores on a plate and groups are weighted by size (Holsinger and Weir 2009). Note that this measure describes *r* within fruiting bodies relative to the population on the plate, while other studies (Gilbert et al. 2012) measure *r* as if the plate was one part of a much larger hypothetical reference population.

We analyzed relatedness data by multiple linear regression using the *lm* command in *R*. Because our estimates of *r* are mathematically bounded between zero and one we used logistically transformed values (ln[*r*/(1–*r*)]), which linearized the relationship with $\log_{10}$(colonizing spores) and homogenized variances. We also analyzed *r* as a function of $\log_{10}$(germinating amoebae), which we estimated as (number of inoculated spores) × (germination rate observed for strain pair in the same experimental replicate). We tested the statistical significance of model parameters using *F* tests comparing the full model to a model lacking the variable of interest. To avoid potentially unreliable estimates of *r*, we excluded a few data points for which the total proportion of *rfp* spores sampled from a plate was >0.9. We also controlled for marker effects by including overall proportion *rfp* as a term in our statistical models.

Density in natural soil populations

To estimate *D. discoideum* density in natural populations, we analyzed previously-published data from small soil cores (6 mm diameter × ~5 mm deep) collected along transects in Mountain Lake Biological Station, Virginia, USA (Fortunato et al. 2003; Gilbert et al. 2012). Samples were collected in the fall, when Dictyostelids are most abundant (Cavender and Raper 1965). Samples were collected in adjacent pairs with small plastic straws, stored at 4° C overnight, suspended in distilled water, and then plated on nutrient media with *Klebsiella pneumoniae*. After 3-5 days incubation, each Dictyostelid plaque typed as *D. discoideum* was counted as an individual isolate.

We calculated the density of *D. discoideum* in these samples as isolate count per cross-section area of the soil core (9π mm^2). We calculated what *r* these colonization densities would create in our experiments using the *predict* command in *R* with the full statistical model and 50% total spores *rfp*. We tested whether isolates were non-uniformly distributed among soil samples using a chi-squared goodness of fit test (*chisq.test* command) with *P* values determined by simulation because expected counts were generally <5. We calculated spatial autocorrelations (Moran's *I*, scaled [-1,1]) of isolate density and presence/absence using the *Moran.I* command in the *ape* package and a Bonferroni correction for multiple comparisons.

Results

Millimeter-scale separation of genotypes can create substantial relatedness within fruiting bodies

To assay how much amoebae disperse while grazing, we spotted amoebae onto bacterial lawns and followed both the outermost visible sign of amoebae among bacteria and the point at which they start aggregating to form fruiting bodies (Fig. 1A). The distance between these two landmarks (here called the plaque boundary) measures how far amoebae disperse between colonizing a feeding site and aggregating to form fruiting bodies. Plaques grew 18.3 (mean ±SD 2.32) mm/day and had boundaries 14.5 (mean ±SD 2.53) mm wide (Fig. 1B). Strain NC34.1 expanded faster than NC28.1 (outer edge v_{max} × background: LR = 16.09, df = 1, P = 0.0001; aggregation boundary v_{max} × background: LR = 8.04, df = 1, P = 0.0046) and had wider boundaries (LR = 11.39, df = 1, P = 0.0007) that themselves expanded faster (LR = 6.10, df = 1, P = 0.0001). Based on these data, a simple expectation might be that fruiting bodies must be separated by one half the distance of a plaque boundary—roughly 7 mm—to draw from different genotype pools.

To directly measure the spatial scale over which intersecting plaques produce mixed-genotype fruiting bodies, we inoculated wild type and *rfp* strains separately 5 cm apart and used flow cytometry to measure the composition of fruiting bodies along a transect connecting the centers of the two resulting plaques. To isolate the effect of spatial separation and exclude any effect caused by strain interactions, we used natural isolates paired with a derivative of the same isolate genetically marked to express red fluorescent protein (*rfp*). Fruiting bodies with substantial proportions of both wild type and *rfp* spores only occurred in a narrow zone a few millimeters wide (Fig. 2). The width of the mixing zone did not differ between strains (LR = 0.410, df = 1, P = 0.52), unlike midpoint location (LR = 3.86, df = 1, P = 0.0495) and maximum proportion *rfp* (LR = 4.90, df = 1, P = 0.027). Amoebae lineages can thus quickly expand across centimeters yet mix very little with other genotypes where plaques intersect.

To assay how strongly colonization density (and thus the average distance between colonizing genotypes) affects the clonality of fruiting bodies, we inoculated bacterial lawns with mixes of isogenic wild type and *rfp* spores (Fig. 3A). We then let amoebae hatch, graze, and create fruiting bodies. At low colonization densities, fluorescent fruiting bodies were clustered in large, visible patches (Fig. 3B). At patch intersections, we observed very few

fruiting bodies with intermediate fluorescence (Fig. 3C). Strongly fluorescent and completely nonfluorescent fruiting bodies were often directly adjacent to each other. At higher densities, fluorescence was more evenly distributed.

We quantified the distribution of wild type and *rfp* spores within and between fruiting bodies on these plates using flow cytometry. At low colonization densities, fruiting bodies contained mostly fluorescent or mostly nonfluorescent spores (Fig. 4A). At high colonization densities, fruiting bodies contained a uniform mix of both. We summarized the genotypic uniformity of cells within fruiting bodies in terms of kin selection relatedness (Hamilton's *r*) measured at the *rfp* locus relative to the whole population on a plate. Increasing colonization density decreased *r* (Fig. 4B; $F_{2,43} = 233.9$, $P < 2.2 \times 10^{-16}$). Over our range of experimental conditions, *r* ranged from ~0.9 to near zero and varied log-logistically with colonization density. Relatedness was > 0.5 when plates were colonized by <0.18 spores/mm^2, equivalent to colonizers occupying circular territories of mean diameter 2.7 mm (Fig. S5). Not all colonizing spores germinated into viable amoebae (Fig. S6A). Accounting for germination rate, relatedness was > 0.5 at densities <0.06–0.15 colonizing amoebae/mm^2 (2.9–4.6 mm diameter territories; Fig. S6B).

The relationship between *r* and colonization density varied among *D. discoideum* genetic backgrounds (Fig. 4B; $F_{1,43} = 21.72$, $P = 3.0 \times 10^{-5}$) even after statistically controlling for germination rate ($F_{1,20} = 6.45$, $P = 0.020$). The full statistical model also included a negative association between *r* and the total proportion of *rfp* spores among sampled fruiting bodies (Fig. S7**;** $F_{1,43} = 12.74$, $P = 9.0 \times 10^{-4}$). This association is expected when mutation or protein degradation (Fig. S3) creates nonfluorescent spores derived from the *rfp* strain, increasing the apparent number of mixed-genotype fruiting bodies in populations with high overall proportion *rfp*.

Soil populations are sparse and patchily distributed at millimeter scales

To test whether spatial separation of colonizers is likely to drive the genetic similarity of cells within fruiting bodies from natural populations, we analyzed data from small soil samples taken in Mountain Lake, Virginia, USA (Fortunato et al. 2003; Gilbert et al. 2012). Using the cross-sectional area of the samples, we calculated *D. discoideum* were present in this population at 0.062 isolates/mm^2 (±0.011 SE; Fig. 5A, Fig. S8A), equivalent to individual cells occupying circular territories of mean diameter 4.5 mm. This cell density is

far too low to support creation of fruiting bodies directly. It may reflect, however, the density at which amoebae colonize feeding sites—when a bolus of bacteria is introduced into soil, for example. In our experiments, which more closely match the bacteria-rich environment of feces, colonization at this density would create mean r = 0.64–0.65, depending on the genetic background (Fig. 4B). Isolates were non-randomly clustered in soil samples (goodness of fit χ^2 = 340.7, P < 0.001; Fig. 5A, Fig. S8B) and showed significant spatial autocorrelation in abundance at millimeter scales (Fig. 5B), suggesting spatial demographics dominated by highly local processes. To account for the possibility that some samples were taken from unsuitable microhabitats, we also calculated density using only those samples from which *D. discoideum* were isolated: 0.156 isolates/mm^2 (±0.017 SE, Fig. 5A), which in our experiments would create r = 0.47–0.53. Because not all colonizing spores in our experiments germinated into amoebae, a better comparison might be to the density of germinating cells (Fig. S6). In our experiments this would be r = 0.48–0.62 for the density among all samples and r = 0.31–0.50 for only those samples with *D. discoideum*. Using similar sampling methods in a Maryland population, Eisenberg (1976) found 18 *D. discoideum* isolates in 101 samples: 0.0063 isolates/mm^2, an order of magnitude less dense than Virginia. By all measures, then, soil populations of amoebae are sparse enough that the high clonality of cells within fruiting bodies can be largely driven by ecological processes that spatially segregate genotypes.

Discussion

To understand the causes of genetic social structure among cooperating microbes, we tested how spatially separated colonizing *D. discoideum* genotypes need to be to produce fruiting bodies consisting mostly of cells from a single clonal lineage. When spores colonize a patch of prey bacteria, amoebae hatch out and actively disperse while grazing, creating plaques that expand centimeters per day with diffuse boundaries centimeters wide. Nevertheless, the fruiting bodies that amoebae eventually create reflect the spatial distribution of genotypes in colonizers. We found that this process can create substantial kin selection relatedness of cells within fruiting bodies when colonizing genotypes are separated on average by only a few millimeters. Even adjacent fruiting bodies can consist of different genotypes. The degree of genetic clonality within fruiting bodies is thus strongly

driven by the population ecology of colonization, growth, and dispersal over spatial scales as small as fruiting bodies themselves.

To assess spatial separation of genotypes in natural populations, we calculated *D. discoideum* densities in soil using previously published field data. Amoebae were sparse and patchily distributed at millimeter scales. The densities we observed in soil were low enough to create substantial clonality in our experimental fruiting bodies through spatial structure alone. The fine-scale spatial structure of cells and genotypes in natural *D. discoideum* populations thus appears to be a potent cause of genetic social structure among cooperating cells. Fruiting bodies grown from field-collected dung are largely clonal, with relatedness at microsatellite loci of r = 0.86–0.99 (Gilbert et al. 2007). The genetic uniformity of fruiting bodies has been considered puzzling, given the heterogeneity of millimeter-scale soil samples (Fortunato et al. 2003; Gilbert et al. 2012). Our results show that spatial separation of genotypes at these millimeter scales can solve this puzzle. The amoebae densities we observed in soil are typical of free-living microbial eukaryotes (Finlay 2002), so fine-scale spatial structure may create relatedness in many other species, as well.

Previous studies have shown that, in principle, low densities can promote selection for cooperative microbes, presumably due to decreased interaction between genotypes (Greig and Travisano 2004; MacLean and Gudelj 2006; Chuang et al. 2009; Ross-Gillespie et al. 2009). With all of these studies, however, there has been no way to compare laboratory results to the conditions microbes experience in natural populations. In some cases, clonality was completely determined by the experimental passaging of cells (e.g. Chuang et al. 2009). Here we have tested whether low colonization density is in fact strong enough to drive clonality in actual microbial populations, and if so, how much. In the process, we have also directly quantified how density affects kin selection relatedness within fruiting bodies, independent of any effect density might also have on the fitness costs and benefits of social traits. Importantly, we used a system where social groups are created by the microbes themselves.

We measured genetic clonality in laboratory-grown fruiting bodies so we could isolate spatial separation's effect independently of other potential factors. From a microbe's point of view, however, natural substrates like soil are complex, heterogeneous habitats that differ in many ways from the flat, wide-open spaces they encounter on agar plates (Young et al. 2008). Many of these differences seem likely to strengthen the effect of spatial

separation. The total surface area of soil, for example, is typically orders of magnitude larger than the simple cross-sectional area of a soil core (Young et al. 2008). Pathways of connectivity on natural substrates are also often winding and tortuous. High water content can increase spatial connectivity for swimming microbes like bacteria (Wolf et al. 2013), but Dictyostelid amoebae adhere to and crawl on surfaces. Our results suggest that the fine-scale spatial structure of these organisms' natural habitats are likely to have important effects on genetic social structure and thus deserve further study in this context.

One might wonder what percentage of *D. discoideum* cells in soil are successfully sampled using standard methods. If some fraction of cells went undetected, our estimates of amoebae density in soil would be underestimates, making different genotypes appear more spatially separated than they really are. Some amoebae genotypes, for example, might not grow on on *Klebsiella* lawns. *D. discoideum* can consume many phylogenetically diverse bacteria (Raper 1937) but can have feeding preferences (DiSalvo et al. 2014). If there were *D. discoideum* strains that did not grow under our experimental conditions, they would be absent not only from the soil density data but also from the previous estimates of genetic diversity in fruiting bodies grown from natural substrates, which used the same culture methods (Gilbert et al. 2007). Such a non-detection bias would therefore affect both the data and the observations we're using the data to explain. Such strains would also be under-counted in both chimeric and clonal fruiting bodies, and so wouldn't be expected to bias *r* in one direction or another. There may be yet other reasons for failing to detect all *D. discoideum* cells in soil. We know of no data available about that address this concern, but our results show that the only process currently known to be capable of creating the high genetic uniformity in natural fruiting bodies is spatial separation of genotypes. Our findings are one of the closest approaches so far to understanding microbial relatedness at scales relevant to cooperation.

Dictyostelid amoebae have genetic kin recognition systems that reduce developmental aggregation with other genotypes (Mehdiabadi et al. 2006; Ostrowski et al. 2008; Benabentos et al. 2009; Hirose et al. 2011; Strassmann et al. 2011). Similar systems have also been found in bacteria such as *Myxococcus xanthus* (Vos and Velicer 2009) and *Proteus mirabilis* (Gibbs et al. 2008). In *D. discoideum*, kin recognition lessens the negative effects of cheaters (Ho et al. 2013) but only weakly increases relatedness within fruiting bodies by $r = 0.05–0.15$ (Gilbert et al. 2012). Its realized effect is likely to be even smaller in natural habitats because spatial separation will reduce opportunities for different genotypes to

come in contact. Available evidence thus does not point to kin recognition being a substantial contributor to the genetic uniformity of *D. discoideum* fruiting bodies.

Another spatial process that can create clonality within fruiting bodies occurs when only those cells on the edge of a colony or plaque reproduce, leading to a form of genetic drift that causes initially mixed genotypes to separate out into distinct sectors (Hallatschek et al. 2007; Nadell et al. 2010; Van Dyken et al. 2013). Colonization density and drift have different effects over the life cycle of a habitat patch. Low colonization density creates an initial amount of spatial distance between genotypes that then decreases as colonies or plaques cells grow together and intermix, while drift can start from a highly mixed state and which then de-mixes with growth. Buttery et al. (2012) investigated spatial drift in *D. discoideum* and found that while it did operate, it required much larger spatial scales (on the order of centimeters) and plateaued at intermediate values. Spatial drift thus seems unlikely to be a major contributor to relatedness in natural populations of *D. discoideum*.

Our results illustrate how population ecology plays an important role in the evolution of microbial cooperation and multicellularity, but in doing so they also call attention to the fact that many aspects of Dictyostelid ecology are still poorly understood. For example, it is unknown how much feces contributes to Dictyostelid population growth relative to bare soil. It is unknown how often amoebae colonize feeding sites directly from soil, are brought by arthropod vectors (Huss 1989; smith et al. 2014), or are already present as spores in animal guts (Suthers 1985). If brought by vectors, feces might be a place where different genotypes are brought together, lowering relatedness compared to soil. It is also unknown if spores colonize feeding sites as clumps from the same fruiting body or if they are separated on the way and colonize as dispersed singletons.

The reason why cells from intersecting plaques don't intermix more is likely in part due to the mechanism of cell aggregation. Starving cells release cAMP and then migrate toward its highest concentration (Loomis 2014). For cells at the edge of an expanding plaque, the highest cAMP concentration would be toward the plaque's interior, where cells began starving earlier, and therefore away from any adjacent plaques. Nevertheless, the fact that plaques have diffuse edges several aggregation territories wide would seem to suggest that genotypes from neighboring plaques would intermix well before starvation. A better understanding of this phenomenon will likely require detailed knowledge of amoebae foraging behavior coupled with a spatially explicit model of plaque growth that

incorporates this knowledge instead of relying on simple reaction-diffusion assumptions (Murray 2003).

In our experiments, the effect of colonization density on the clonality of fruiting bodies varied with genetic background, indicating heritable variation in traits (such as dispersal while grazing) that affect how often cells interact with other genotypes. This illustrates the fact that, because social structure is influenced by dispersal and grouping behavior, relatedness is also in part a biological trait that can itself evolve (Le Galliard et al. 2005; Hochberg et al. 2008; Powers et al. 2011).

Conclusions

To understand when microbes evolve to cooperate or to cheat, we must identify what processes determine the extent to which different genotypes interact. Our results show how the genetic social structure of a microbial model system is driven by the population ecology of colonization, growth, and dispersal acting at millimeter scales. Our results support extensive theoretical work showing that social evolution in spatially structured populations strongly depends on ecological details like dispersal, habitat saturation, and the scale of population regulation (Platt and Bever 2009; Lehmann and Rousset 2010) and add to a growing body of evidence that population ecology plays a particularly key role in microbial cooperation (Brockhurst et al. 2007; Brockhurst et al. 2008; Brockhurst et al. 2010; Datta et al. 2013). Because medically important microbial traits like virulence and antimicrobial resistance often have a social component (West et al. 2007; Raymond et al. 2012; Diard et al. 2013; Yurtsev et al. 2013; Leggett et al. 2014), understanding how ecological and genetic processes in these systems spatially structure genotypes at fine spatial scales may help us better control the proliferation of undesirable microbes.

Acknowledgments

We thank A. Wen and J. Masi for laboratory assistance, D. Duncan for microscopy assistance, K. Geist for statistical advice, and J. Myers for discussion. This material is partly based upon work supported by the National Science Foundation under Grant Nos. DEB1204352, IOS1256416, and DEB1146375 to JES and DCQ.

Conflict of interest statement

The authors declare that they have no competing commerical interest in relation to this work.

Author contributions

js conceived the study. All authors contributed to experimental design. js performed the experiments and analyzed the data with feedback from DCQ and JES. js wrote the first draft. DCQ and JES contributed additional edits to the text. All authors read and approved the final manuscript.

Literature cited

Benabentos, R., S. Hirose, R. Sucgang, T. Curk, M. Katoh, E. A. Ostrowski, J. E. Strassmann, D. C. Queller, B. Zupan, G. Shaulsky, and A. Kuspa. 2009. Polymorphic members of the *lag* gene family mediate kin discrimination in *Dictyostelium*. Curr. Biol. 19:567-572.

Brockhurst, M. A., A. Buckling, and A. Gardner. 2007. Cooperation peaks at intermediate disturbance. Curr. Biol. 17:761-765.

Brockhurst, M. A., A. Buckling, D. Racey, and A. Gardner. 2008. Resource supply and the evolution of public-goods cooperation in bacteria. BMC Biol. 6:20.

Brockhurst, M. A., M. G. J. L. Habets, B. Libberton, A. Buckling, and A. Gardner. 2010. Ecological drivers of the evolution of public-goods cooperation in bacteria. Ecology 91:334-340.

Buttery, N. J., C. N. Jack, B. Adu-Oppong, K. T. Snyder, C. R. L. Thompson, D. C. Queller, and J. E. Strassmann. 2012. Structured growth and genetic drift raise relatedness in the social amoeba *Dictyostelium discoideum*. Biol. Lett. 8:794-797.

Buttery, N. J., D. E. Rozen, J. B. Wolf, and C. R. L. Thompson. 2009. Quantification of social behavior in *D. discoideum* reveals complex fixed and facultative strategies. Curr. Biol. 19:1373-1377.

Cavender, J. C., and K. B. Raper. 1965. The Acrasiae in nature. II. Forest soil as a primary habitat. . Am. J. Bot. 52:297-302.

Datta, M. S., K. S. Korolev, I. Cvijovic, C. Dudley, and J. Gore. 2013. Range expansion promotes cooperation in an experimental microbial metapopulation. Proc. Natl. Acad. Sci. USA 110:7354-7359.

Diard, M., V. Garcia, L. Maier, M. N. P. Remus-Emsermann, R. R. Regoes, M. Ackermann, and W.-D. Hardt. 2013. Stabilization of cooperative virulence by the expression of an avirulent phenotype. Nature 494:353-356.

Dimitriu, T., C. Lotton, J. Bénard-Capelle, D. Misevic, S. P. Brown, A. B. Lindner, and F. Taddei. 2014. Genetic information transfer promotes cooperation in bacteria. Proc. Natl. Acad. Sci. USA 111:11103-11108.

DiSalvo, S., D. A. Brock, j. smith, D. C. Queller, and J. E. Strassmann. 2014. In the social amoeba, *Dictyostelium discoideum*, density, not farming status, determines predatory success on unpalatable *Escherichia coli*. BMC Microbiol 14:328.

Eisenberg, R. M. 1976. Two-dimensional microdistribution of cellular slime molds in forest soil. Ecology 57:380-384.

Ennis, H. L., D. N. Dao, S. U. Pukatzki, and R. H. Kessin. 2000. *Dictyostelium* amoebae lacking an F-box protein form spores rather than stalk in chimeras with wild type. Proc. Natl. Acad. Sci. USA 97:3292-3297.

Finlay, B. J. 2002. Global dispersal of free-living microbial eukaryote species. Science 296:1061-1063.

Fortunato, A., J. E. Strassmann, L. Santorelli, and D. C. Queller. 2003. Co-occurrence in nature of different clones of the social amoeba, *Dictyostelium discoideum*. Mol. Ecol. 12:1031-1038.

Francis, D., and R. Eisenberg. 1993. Genetic structure of a natural population of *Dictyostelium discoideum*, a cellular slime mould. Mol. Ecol. 2:385-391.

Gentleman, R., V. Carey, D. Bates, B. Bolstad, M. Dettling, S. Dudoit, B. Ellis, L. Gautier, Y. Ge, J. Gentry, K. Hornik, T. Hothorn, W. Huber, S. Iacus, R. Irizarry, F. Leisch, C. Li, M. Maechler, A. Rossini, G. Sawitzki, C. Smith, G. Smyth, L. Tierney, J. Yang, and J. Zhang. 2004. Bioconductor: open software development for computational biology and bioinformatics. Genome Biol. 5:R80.

Gibbs, K. A., M. L. Urbanowski, and E. P. Greenberg. 2008. Genetic determinants of self identity and social recognition in bacteria. Science 321:256-259.

Gilbert, O. M., K. R. Foster, N. J. Mehdiabadi, J. E. Strassmann, and D. C. Queller. 2007. High relatedness maintains multicellular cooperation in a social amoeba by controlling cheater mutants. Proc. Natl. Acad. Sci. USA 104:8913-8917.

Grafen, A. 1985. A geometric view of relatedness. Oxford. Surv. Evol. Biol. 2:28-89.

Hamilton, W. D. 1964. Genetical evolution of social behaviour, I and II. J. Theor. Biol. 7:1-52.

Hirose, S., R. Benabentos, H.-I. Ho, A. Kuspa, and G. Shaulsky. 2011. Self-recognition in social amoebae is mediated by allelic pairs of tiger genes. Science 333:467-470.

Hochberg, M. E., D. J. Rankin, and M. Taborsky. 2008. The coevolution of cooperation and dispersal in social groups and its implications for the emergence of multicellularity. BMC Evol. Biol. 8:238.

Holsinger, K. E., and B. S. Weir. 2009. Genetics in geographically structured populations: defining, estimating and interpreting FST. Nat. Rev. Genet. 10:639-650.

Huss, M. J. 1989. Dispersal of cellular slime molds by two soil invertebrates. Mycologia 81:677-682.

Kuzdzal-Fick, J. J., S. A. Fox, J. E. Strassmann, and D. C. Queller. 2011. High relatedness Is necessary and sufficient to maintain multicellularity in *Dictyostelium*. Science 334:1548-1551.

Le Galliard, J. F., R. Ferriere, and U. Dieckmann. 2005. Adaptive evolution of social traits: origin, trajectories, and correlations of altruism and mobility. Am. Nat. 165:206-224.

Lehmann, L., and F. Rousset. 2010. How life history and demography promote or inhibit the evolution of helping behaviours. Phil. Trans. Roy. Soc. B: Biol. Sci. 365:2599-2617.

Loomis, W. F. 2014. Cell signaling during development of *Dictyostelium*. Dev. Biol. 391:1-16.

Mehdiabadi, N. J., C. N. Jack, T. T. Farnham, T. G. Platt, S. E. Kalla, G. Shaulsky, D. C. Queller, and J. E. Strassmann. 2006. Kin preference in a social microbe. Nature 442:881-882.

Murray, J. D. 2003. Mathematical Biology. Springer, Berlin.

Ostrowski, E. A., M. Katoh, G. Shaulsky, D. C. Queller, and J. E. Strassmann. 2008. Kin discrimination increases with genetic distance in a social amoeba. PLoS Biol. 6:2376-2382.

Pang, K. M., M. A. Lynes, and D. A. Knecht. 1999. Variables controlling the expression level of exogenous genes in *Dictyostelium*. Plasmid 41:187-197.

Parkinson, K., N. J. Buttery, J. B. Wolf, and C. R. L. Thompson. 2011. A simple mechanism for complex social behavior. PLoS Biol. 9:e1001039.

Pepper, J. W. 2000. Relatedness in trait group models of social evolution. J. Theor. Biol. 206:355-368.

Platt, T. G., and J. D. Bever. 2009. Kin competition and the evolution of cooperation. Trends Ecol. Evol. 24:370-377.

Pollitt, E. J., S. A. West, S. A. Crusz, M. N. Burton-Chellew, and S. P. Diggle. 2014. Cooperation, quorum sensing, and evolution of virulence in *Staphylococcus aureus*. Infect. Immun. 82:1045-1051.

Powers, S. T., A. S. Penn, and R. A. Watson. 2011. The concurrent evolution of cooperation and the population structures that support it. Evolution 65:1527-1543.

Queller, D. C. 1992. A general model for kin selection. Evolution 46:376-380.

Queller, D. C., and K. F. Goodnight. 1989. Estimating relatedness using genetic markers. Evolution 43:258-275.

Raper, K. R. 1937. Growth and development of *Dictyostelium discoideum* with different bacterial associates. Journal of Agricultural Research 55:289-316.

Raymond, B., S. A. West, A. S. Griffin, and M. B. Bonsall. 2012. The dynamics of cooperative bacterial virulence in the field. Science 337:85-88.

Santorelli, L. A., C. R. L. Thompson, E. Villegas, J. Svetz, C. Dinh, A. Parikh, R. Sucgang, A. Kuspa, J. E. Strassmann, D. C. Queller, and G. Shaulsky. 2008. Facultative cheater mutants reveal the genetic complexity of cooperation in social amoebae. Nature 451:1107-1110.

smith, j., D. C. Queller, and J. E. Strassmann. 2014. Fruiting bodies of the social amoeba *Dictyostelium discoideum* increase spore transport by *Drosophila*. BMC Evol. Biol. 14:105.

smith, j., J. D. Van Dyken, and P. C. Zee. 2010. A generalization of Hamilton's rule for the evolution of microbial cooperation. Science 328:1700-1703.

Strassmann, J. E., O. M. Gilbert, and D. C. Queller. 2011. Kin discrimination and cooperation in microbes. Annu. Rev. Microbiol. 65:349-367.

Strassmann, J. E., and D. C. Queller. 2011. Evolution of cooperation and control of cheating in a social microbe. Proc. Natl. Acad. Sci. USA 108:10855-10862.

Strassmann, J. E., Y. Zhu, and D. C. Queller. 2000. Altruism and social cheating in the social amoeba *Dictyostelium discoideum*. Nature 408:965-967.

Suthers, H. B. 1985. Ground-feeding migratory songbirds as cellular slime mold distribution vectors. Oecologia 65:526-530.

Vos, M., and G. J. Velicer. 2009. Social conflict in centimeter and global-scale populations of the bacterium *Myxococcus xanthus*. Curr. Biol. 19:1763-1767.

Waddell, D. R. 1982. The spatial pattern of aggregation centres in the cellular slime mould. Journal of Embryology and Experimental Morphology 70:75-98.

West, S. A., K. Winzer, A. Gardner, and S. P. Diggle. 2012. Quorum sensing and the confusion about diffusion. Trends Microbiol. 20:586-594.

Wolf, A. B., M. Vos, W. de Boer, and G. A. Kowalchuk. 2013. Impact of matric potential and pore size distribution on growth dynamics of filamentous and non-filamentous soil bacteria. PLoS ONE 8:e83661.

Young, I. M., J. W. Crawford, N. Nunan, W. Otten, A. Spiers, and L. S. Donald. 2008. Microbial Distribution in Soils: Physics and Scaling. Pp. 81-121. Advances in Agronomy. Academic Press.

Figure legends

Figure 1. *D. discoideum* cells can disperse centimeters in the time between colonizing a feeding site and aggregating to form fruiting bodies. **(A)** Dictyostelid plaque morphology. Plaques of amoebae grazing on bacterial lawns have an outer ring of dispersing amoebae surrounding an inner region where amoebae aggregate and make fruiting bodies. **(B)** Growth of *D. discoideum* plaques on lawns of *K. pneumoniae* bacteria. Black: radius of outer feeding edge (outermost visible sign of amoebae among bacteria). Grey: radius at which amoebae begin aggregating. Panels show strains. Lines within panels are independent experimental replicates.

Figure 2. Narrow zone of mixed-genotype fruiting bodies where plaques intersect. Points: proportion *rfp* spores in individual fruiting bodies along transect connecting centers of two plaques placed 5 cm apart. Lines: best-fit logistic curves for data from each of four replicate plates. Curves asymptote at ~0.9 due to fluorescence loss. Panels: strain pairs isogenic save for *rfp* marker.

Figure 3. Limited dispersal of amoebae during vegetative growth leaves genotypes spatially segregated over scales as small as individual fruiting bodies. **(A)** Experimental assay. *D. discoideum* spores inoculated onto lawns of bacteria hatched into amoebae, grazed, reproduced asexually, and created fruiting bodies. Inocula included mixture of spores from natural *D. discoideum* isolate and its *rfp*-marked derivative. Amoebae dispersed while grazing, creating diffuse plaques of clonal cells. Where plaques intersected, cells could produce fruiting bodies containing both genotypes. **(B)** Lawns inoculated at low densities contained large, visible patches of wild-type or *rfp* fruiting bodies. At higher densities, fluorescence was more evenly distributed. Images: false-color composite panorama. Edge of 95 mm diameter plates included for scale. **(C)** At patch boundaries, very few fruiting bodies showed intermediate fluorescence. Images: false-color composite from plates inoculated at 0.018 spores/mm^2. For separate white light and fluorescent images see Fig. S4.

Figure 4. Spatial density of colonization strongly determines the statistical similarity of genotypes of within fruiting bodies. **(A)** At low colonization density, fruiting bodies

contained mostly fluorescent or mostly nonfluorescent spores. At high colonization density, all fruiting bodies contained a uniform mix of genotypes. Points show proportion *rfp* spores in individually sampled fruiting bodies (n = 11–12) from five plates each colonized at a different density. Strains: NC28.1 + NC28.1 *rfp*. **(B)** Genotypic similarity of cells within fruiting bodies measured as kin selection relatedness (Hamilton's r) at *rfp* locus relative to all fruiting bodies on a plate. Dotted lines indicates density observed in soil. Points: independent replicate plates. Lines: marginal fit of statistical model at 50% total spores *rfp*. Panels: strain pairs isogenic save for *rfp* marker.

Figure 5. In natural soil populations, *D. discoideum* are sparse and patchily distributed at millimeter scales. **(A)** Isolate density in 6 mm diameter soil cores. **(B)** Spatial autocorrelation of isolate abundance among samples separated by different distances. Shaded area: 95% confidence interval under null hypothesis of no correlation. Star: after correcting for multiple comparisons, the only significant autocorrelation was among samples separated by 6 mm.

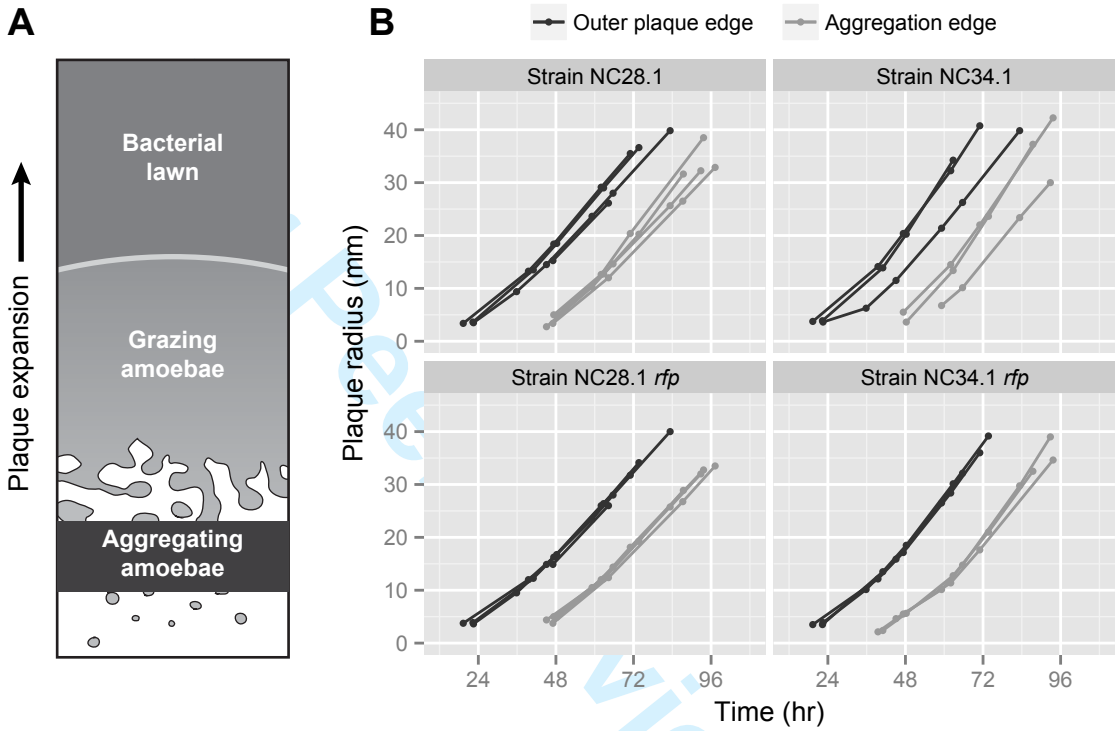

Figure 1. *D. discoideum* cells can disperse centimeters in the time between colonizing a feeding site and aggregating to form fruiting bodies. **(A)** Dictyostelid plaque morphology. Plaques of amoebae grazing on bacterial lawns have an outer ring of dispersing amoebae surrounding an inner region where amoebae aggregate and make fruiting bodies. **(B)** Growth of *D. discoideum* plaques on lawns of *K. pneumoniae* bacteria. Black: radius of outer feeding edge (outermost visible sign of amoebae among bacteria). Grey: radius at which amoebae begin aggregating. Panels show strains. Lines within panels are independent experimental replicates.

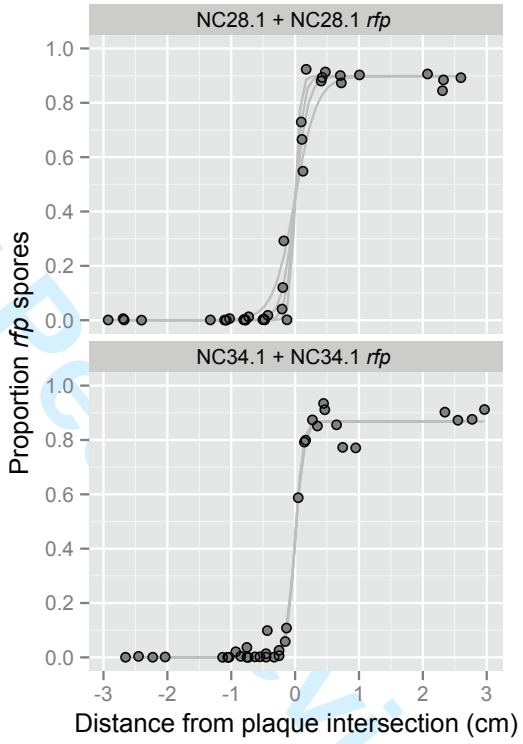

Figure 2. Narrow zone of mixed-genotype fruiting bodies where plaques intersect. Points: proportion *rfp* spores in individual fruiting bodies along transect connecting centers of two plaques placed 5 cm apart. Lines: best-fit logistic curves for data from each of four replicate plates. Curves asymptote at ~0.9 due to fluorescence loss. Panels: strain pairs isogenic save for rfp marker.

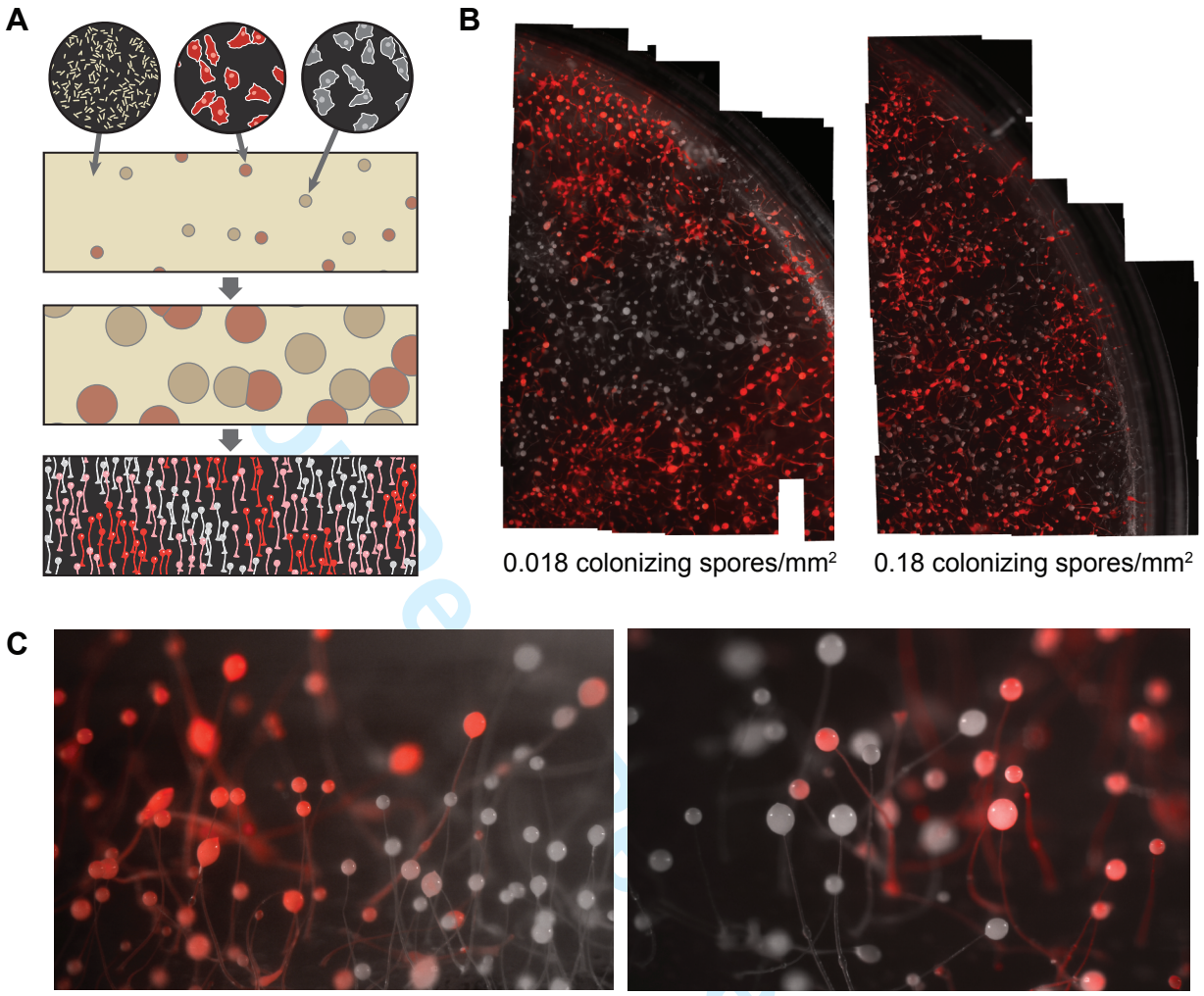

Figure 3. Limited dispersal of amoebae during vegetative growth leaves genotypes spatially segregated over scales as small as individual fruiting bodies. **(A)** Experimental assay. *D. discoideum* spores inoculated onto lawns of bacteria hatched into amoebae, grazed, reproduced asexually, and created fruiting bodies. Inocula included mixture of spores from natural *D. discoideum* isolate and its *rfp*-marked derivative. Amoebae dispersed while grazing, creating diffuse plaques of clonal cells. Where plaques intersected, cells could produce fruiting bodies containing both genotypes. **(B)** Lawns inoculated at low densities contained large, visible patches of wild-type or rfp fruiting bodies. At higher densities, fluorescence was more evenly distributed. Images: false-color composite panorama. Edge of 95 mm diameter plates included for scale. **(C)** At patch boundaries, very few fruiting bodies showed intermediate fluorescence. Images: false-color composite from plates inoculated at 0.018 spores/mm^2. For separate white light and fluorescent images see Figure S4.

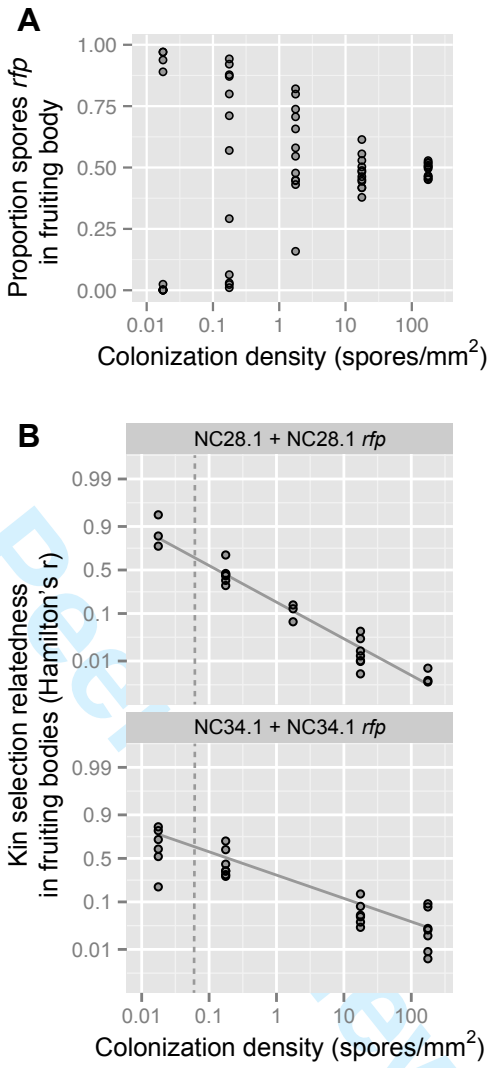

Figure 4. Spatial density of colonization strongly determines the statistical similarity of genotypes of within fruiting bodies. **(A)** At low colonization density, fruiting bodies contained mostly fluorescent or mostly nonfluorescent spores. At high colonization density, all fruiting bodies contained a uniform mix of genotypes. Points show proportion *rfp* spores in individually sampled fruiting bodies (n = 11–12) from five plates each colonized at a different density. Strains: NC28.1 + NC28.1 *rfp*. **(B)** Genotypic similarity of cells within fruiting bodies measured as kin selection relatedness (Hamilton's *r*) at *rfp* locus relative to all fruiting bodies on a plate. Dotted lines indicate density observed in soil. Points: independent replicate plates. Lines: marginal fit of statistical model at 50% total spores *rfp*. Panels: strain pairs isogenic save for *rfp* marker.

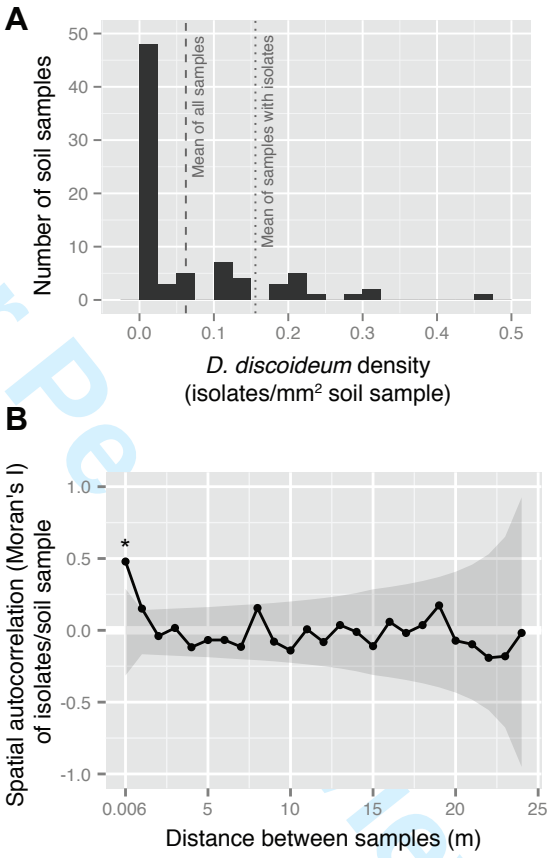

Figure 5. In natural soil populations, *D. discoideum* are sparse and patchily distributed at millimeter scales. **(A)** Isolate density in 6 mm diameter soil cores. **(B)** Spatial autocorrelation of isolate abundance among samples separated by different distances. Shaded area: 95% confidence interval under null hypothesis of no correlation. Star: after correcting for multiple comparisons, the only significant autocorrelation was among samples separated by 6 mm.

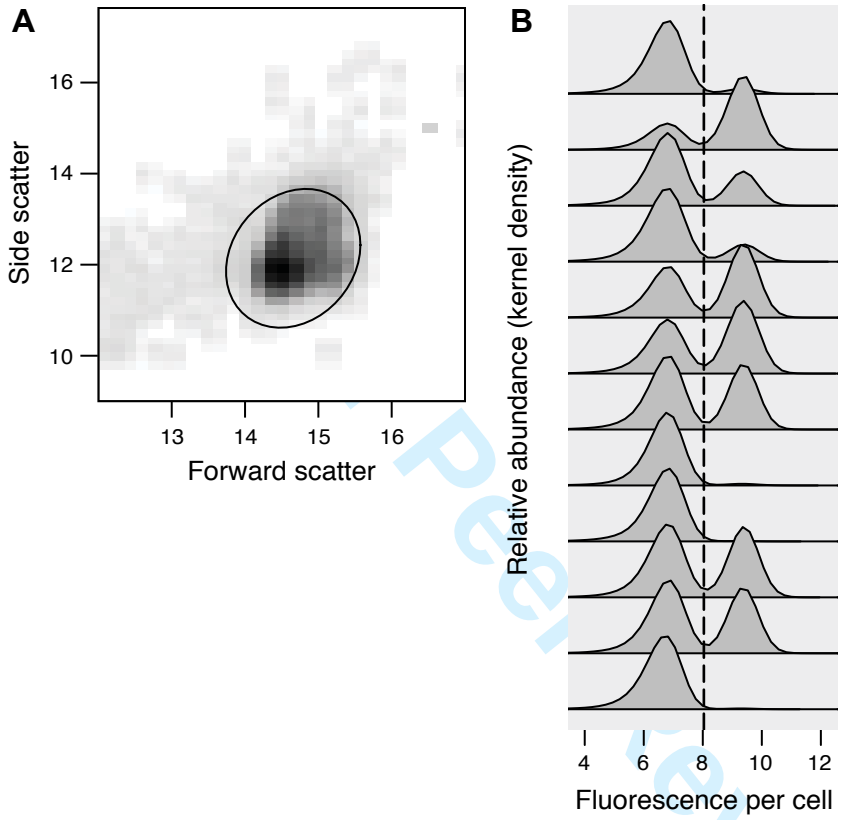

Figure S1. Example flow cytometry data and analysis from one replicate of the NC28.1 + NC28.1 *rfp* strain pair. **(A)** *D. discoideum* spores are isolated from debris by fitting a bivariate normal distribution to forward scatter/side scatter data in the region where *Dictyostelium* cells are expected, then including all events within two standard deviations (oval). Data show spores from a single fruiting body **(B)** Spores are algorithmically divided into wild type and *rfp* populations (dashed line) based on distribution of fluorescence among cells isolated from individual fruiting bodies on the same plate. Data show distribution of fluorescence among cells from 12 separate fruiting bodies.

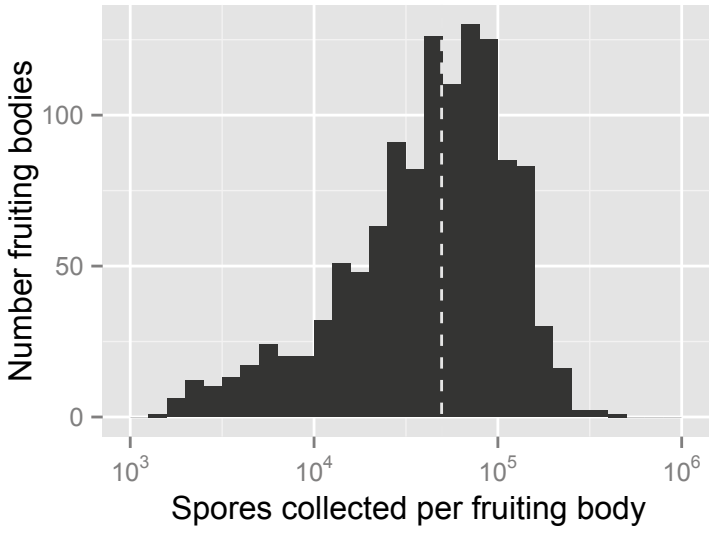

Figure S2. Distribution of fruiting body sizes as measured by number of collected spores. Data include all strains and colonization densities in spatial structure assay (*n* = 1200 fruiting bodies).

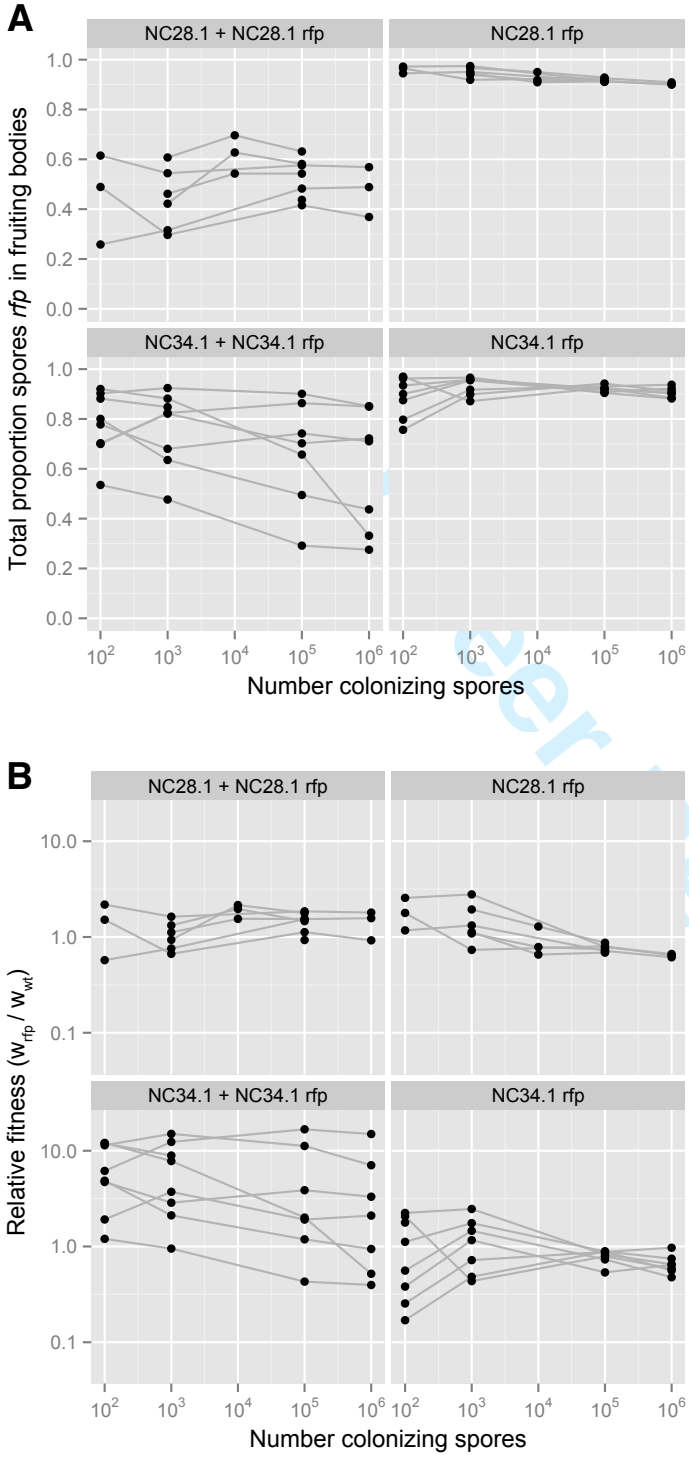

Figure S3. Stability and fitness effects of the *rfp* marker. Points show data from individual plates. Lines connect data from the same experimental block, derived from the same pool of colonizers. **(A)** Total proportion spores *rfp* in fruiting bodies from relatedness assays and from all-*rfp* control experiments. By themselves, *rfp* strains typically expressed fluorescence in >90% of collected spores. In mixes, consistency among plates within replicates (roughly horizontal lines) suggests that most deviation from 50:50 *rfp*:*wt* was caused by variation in the initial proportion among colonizers rather than loss and selection on lawns. **(B)** Relative fitness of *rfp*, calculated as $v = q'/(1-q')/(q/(1-q))$, where q is the initial frequency of *rfp* among colonizing spores and q' is *rfp* frequency among spores in fruiting bodies. The largest change in *rfp* frequency over the course of the assay was the increase in mixes with NC34.1, likely due to that strain's sometimes-low germination rate (Fig. S6).

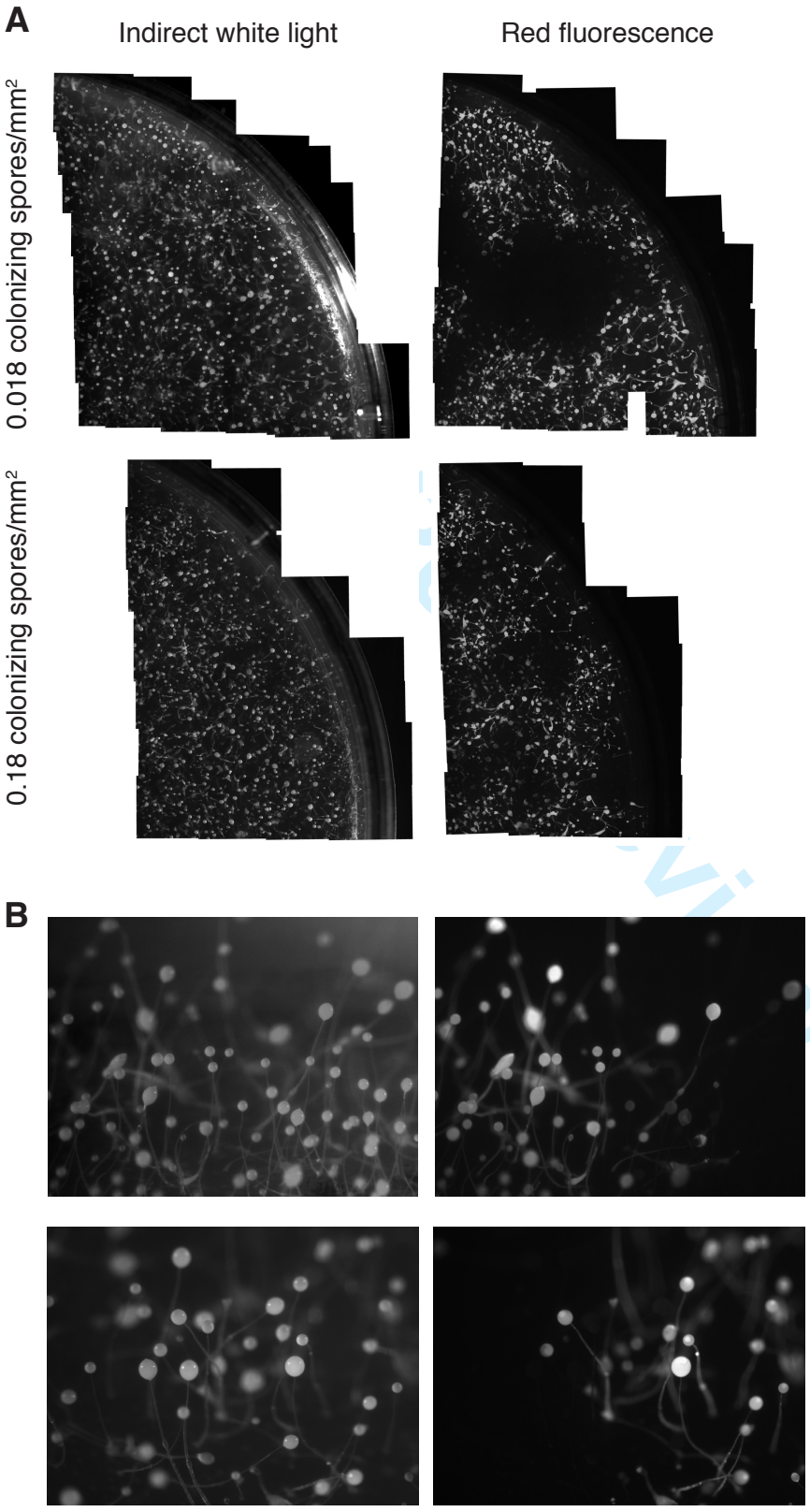

Figure S4. Separate white light and red fluorescent images of spatially genetic structure in fruiting bodies. **(A)** Spatial distribution of NC28.1 and NC28.1 *rfp* cells on plates inoculated at 0.018 spores/mm^2 (10^2 spores/plate) or 0.18 spores/mm^2 (10^3 spores/plate). Images show composite panoramas made from 26-52 separate stereomicroscope images. Edge of 95 mm diameter plate included for scale. **(B)** At plaque intersections, very few fruiting bodies contain both wild type and *rfp* cells at substantial frequencies. Images show fruiting bodies at the intersection of wild type and *rfp* plaques on plates inoculated with 0.018 spores/mm^2 (100 spores/plate) of strains NC28.1 and NC28.1 *rfp*.

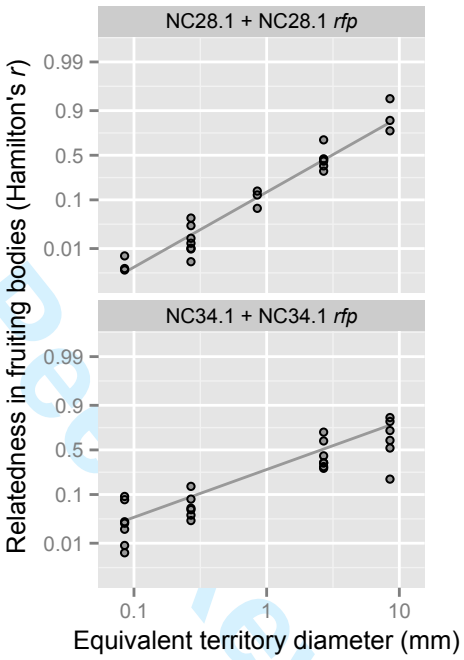

Figure S5. Relatedness within fruiting bodies as a function of colonization density, here plotted as the diameter of an equivalent circular territory with the same area per colonizing spore. Points: independent replicate plates. Lines: marginal fit of statistical model at 50% total spores *rfp*. Panels: strain pairs isogenic save for *rfp* marker.

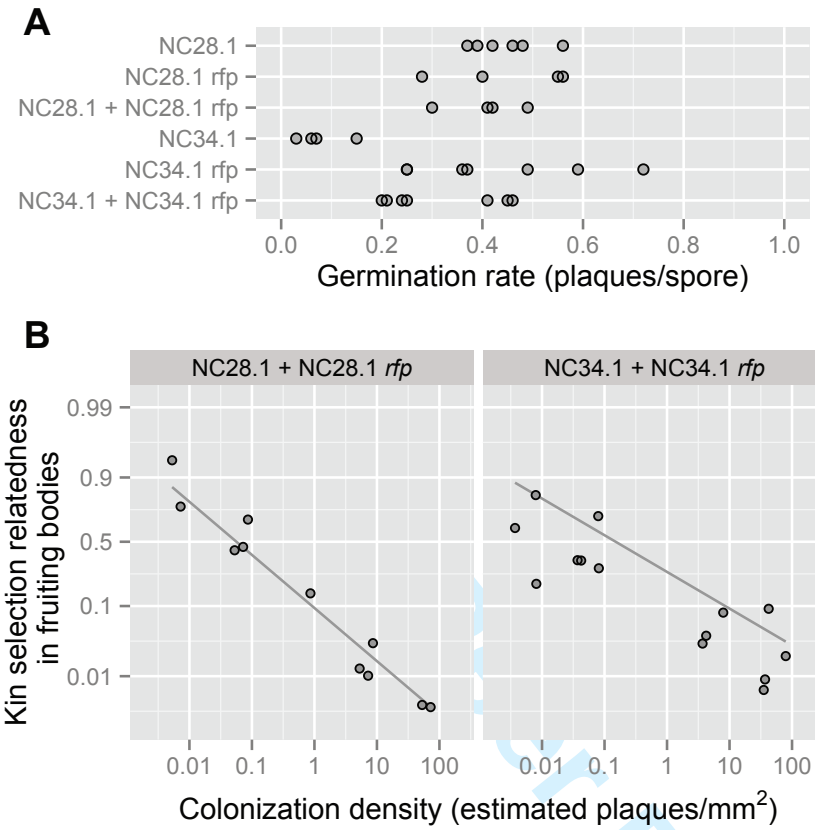

Figure S6. **(A)** Germination rate of colonizing spores. Data show number of plaques observed on bacterial lawns inoculated with 100 spores. **(C)** Relatedness as function of colonizing amoebae (inoculated spores x germination rate). Points show independent replicate plates. Lines show marginal fit of full statistical model at 50% total spores *rfp*.

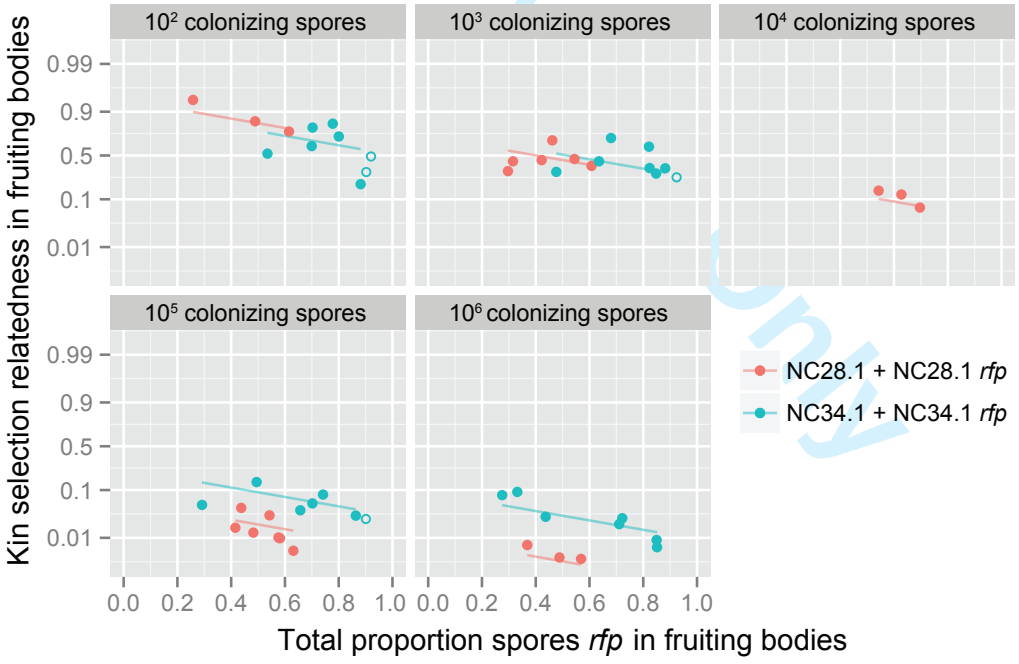

Figure S7. Negative association between relatedness and total proportion *rfp* spores among sampled fruiting bodies. Solid points: Independent replicate plates. Lines: Fitted statistical model. Open points: data where total proportion *rfp* > 0.9, excluded to avoid potentially unreliable relatedness estimates.

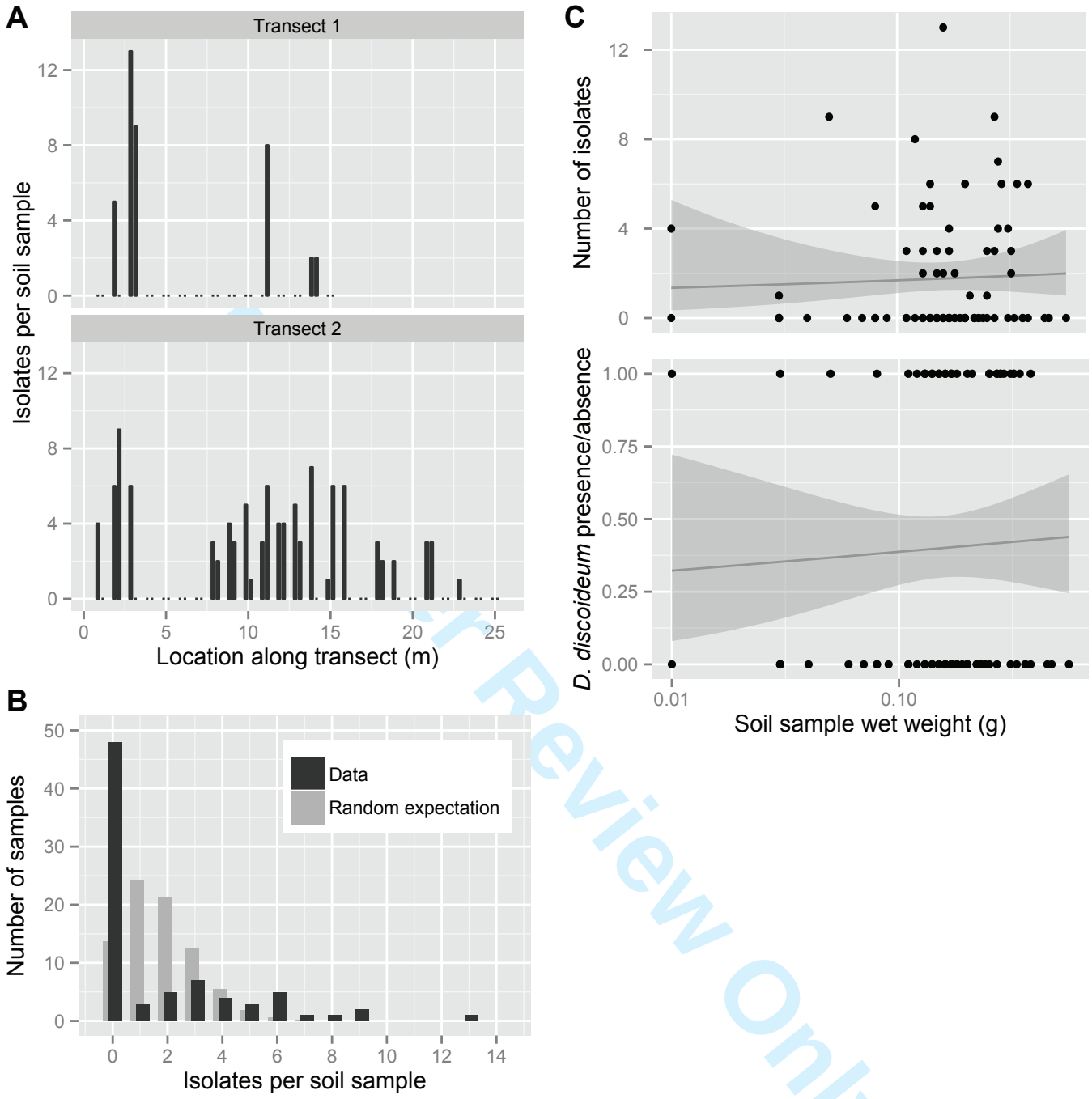

Figure S8. Spatial distribution of *D. discoideum* in a natural population. **(A)** Distribution of isolates from paired soil samples along two transects in Mountain Lake, VA, USA. **(B)** Isolates are clustered among samples. Black bars show observed distribution of isolate densities. Grey bars show expected Poisson distribution under uniform mean density. **(C)** Mass of soil samples not significantly associated with isolate abundance (Spearman $\rho = 0.059$, $S = 80276$, $P = 0.60$, two-sided; quassipoisson GLM $\chi^2_1 = 0.13$, $P = 0.86$) or probability of isolating *D. discoideum* (binomial GLM $\chi^2_1 = 0.023$, $P = 0.88$). Points show samples. Lines and shaded area show fit and 95% confidence interval of generalized linear models.